

**Short Communication**

**Characterization of Cobalt Oxide  $\text{Co}_3\text{O}_4$  Nanoparticles Prepared by Various Methods: Effect of Calcination Temperatures on Size, Dimension and Catalytic Decomposition of Hydrogen Peroxide**

S. L. Sharifi<sup>1\*</sup>, H. R. Shakur<sup>2</sup>, A. Mirzaei<sup>1</sup>, A. Salmani<sup>1</sup>, M. H. Hosseini<sup>1</sup>

1- Chemistry Department of Imam Hussein University, Tehran, I. R. Iran

2- Physics Department of Imam Hussein University, Tehran, I. R. Iran

(\*) Corresponding author: slsharifi@yahoo.com

(Received: 10 Dec. 2012 and Accepted: 23 March 2013)

**Abstract:**

*In this scientific research work we report a novel method to synthesis  $\text{Co}_3\text{O}_4$  nanoparticles via calcinations of cobalt hydroxide which can be conveniently prepared by the  $\text{Co}(\text{NO}_3)_2 \cdot 6\text{H}_2\text{O}$  with different reactants. In order to study the effect of calcination temperature on structure and morphology of the nanoparticles, the calcinations take place at various temperatures (at 300°C, 500°C and 700°C). The nature of cobalt oxide species depending on heat treatment. The samples at low temperature show decrease on size and dimension. The characteristics of the nanoparticles were investigated by XRD patterns, IR spectroscopy and scanning electron microscopy (SEM). It indicates that at higher temperature, greater nanoparticles were produced. Decomposition of  $\text{H}_2\text{O}_2$  showed that calcination at 300°C result to higher activity.*

**Keywords:** Cobalt oxide, Microemulsions, Nanoparticles, Hydrogen peroxide, Calcination temperatures.

**1. INTRODUCTION**

Transition metal oxide have many applications of interesting properties arising due to their variable oxidation state [1]. Cobalt oxide  $\text{Co}_3\text{O}_4$  is an important transition metal oxide because of its application in various field of research and industry include pigments, gas sensor, magnetic materials, catalyst, anode materials for rechargeable Li-batteries, electrochromic devices, electrochemical systems and high-temperature solar selective absorbers [2-12].

The difference in oxygen defect, oxygen holes and oxygen adsorbed in different state of cobalt in  $\text{Co}_3\text{O}_4$  (a mixed valance material that is formally

$\text{Co}^{\text{II}} \text{Co}^{\text{III}} \text{O}_4$ ) [13] are thought to be the reason for high activity and selectivity of this metal oxide catalysts [12].

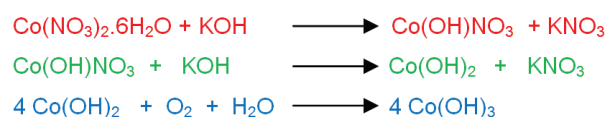
Therefore, in this field a variety of methods have been reported for preparing  $\text{Co}_3\text{O}_4$  such as the thermal decomposition of cobalt precursors under oxidizing condition (210-815°C) [7, 14-19], chemical spray pyrolysis (300-400°C) [4, 20-23], chemical vapor deposition (CVD) [24], sol-gel [25, 26], microemulsion [1, 16], solvo thermal [27], hard templating [14], hydrothermal [3, 11], mechanochemical [2] and chemical combustion [28]. Nevertheless, all of the above physical and chemical methods need some special instruments and harsh conditions. In this paper we report

different methods and procedures with their morphology, discuss their X-Ray pattern and IR spectra. However to the best of our knowledge, there has been no report on the preparation of spinel-type  $\text{Co}_3\text{O}_4$  nanoparticles via cobalt hydroxide obtained from cobalt nitrate and potassium hydroxide in aqueous media and from reverse micellar method with PVP as surfactant. However we report a novel precipitation method that is more facile, easy, simple and effective to synthesis  $\text{Co}_3\text{O}_4$  nanoparticles that have not been reported in the literatures.

## 2. EXPERIMENTAL

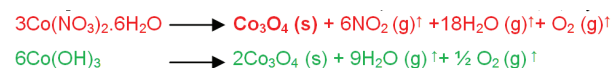
### 2.1. Synthesis (Sample preparation)

In the method I cobalt nitrate  $\text{Co}(\text{NO}_3)_2 \cdot 6\text{H}_2\text{O}$  (0.6 M) was dissolved in 100 ml. deionized water. Then 100 ml. KOH aqueous solutions (3.2 M) were added drop wise to the precursor solution. Pink precipitate appeared immediately which easily to oxidized by air and low heat or weak oxidizing agents to  $\text{Co}(\text{OH})_3$ . The dark brown precipitate was separated and washed with deionized water and dried in an oven at  $110^\circ\text{C}$  for 20 hours. The dried cobalt hydroxide was ground and preserved in a desiccator.



For the preparation of cobaltic-cobaltous oxide  $\text{Co}_3\text{O}_4$ , the dark brown cobaltic hydroxide was heated at  $300^\circ\text{C}$ ,  $500^\circ\text{C}$  and  $700^\circ\text{C}$  for 3-4 hours.

In the method II cobalt nitrate and cobalt (III) hydroxide separately were weighed (5gr.) and ground to a preferred size and then transferred into two different crucibles and exposed to microwave energy (600W) in a microwave oven for 20 minutes. At the end of the experiment, the samples were allowed to cool inside the oven. The microwave-assisted decomposition reaction of cobalt nitrate hexahydrate and cobalt (III) hydroxide represented as follow:



During microwave radiation a decomposition reaction took place and caused  $\text{NO}_2$  and  $\text{O}_2$  gases to be released from the cobalt nitrate sample.

In the method III the synthesis of cobalt oxide utilized two microemulsions. Micro emulsion (a) composed of polyvinylpyrrolidone (PVP) as surfactant, n-butanol as the hydrocarbon phase, and 5% cobalt nitrate solution as the aqueous phase. Microemulsion (b) had the same constituents as microemulsion (a) except that the aqueous phase was a solution of ammonium nitrate (2.5%) instead of cobalt nitrate. The weight fractions of various constituents in these microemulsions were as follows:

19% of PVP, 13% of the aqueous phase and 68% of n-butanol [1]. These two microemulsions were mixed slowly and stirred for 5 hours on a magnetic stirrer. The resulting precipitate was separated from the polar solvent and surfactant by centrifugation with 8000 rpm/min in 30 minutes. The precipitate washed for several times and was dried in air and then heated at  $300^\circ\text{C}$  for 24 hours to obtain cobalt oxide  $\text{Co}_3\text{O}_4$  nanoparticles.

### 2.2. Catalytic decomposition of $\text{Co}_3\text{O}_4$ calcined at different temperature

$\text{H}_2\text{O}_2$  undergoes an exothermic reaction to form  $\text{O}_2$  and  $\text{H}_2\text{O}$ . ( $\text{H}_2\text{O}_2 \rightarrow \text{H}_2\text{O} + \text{O}_2$ )

In this paper, the decomposition of hydrogen peroxide, was studied with catalyst  $\text{Co}_3\text{O}_4$  with concentration of 5% at room temperature. Catalytic measurements were carried out by using the gasometric technique about 0.1g of the catalyst was added to a known amount of hydrogen peroxide (10 ml, 5%v/v) taken in a closed reaction vessel and the contents were stirred at 313 K. The volume of oxygen evolved was measured at regular time intervals.

### 2.3. Characterization

X-ray powder diffraction (XRD) were recorded using Scifert3003TT, X-ray diffractometer with high density Cu  $\text{K}\alpha$  radiation ( $\lambda=1.54^\circ\text{A}$ ). The IR-spectrometer was taken on Perkin-Elmer 783 with sample as KBr disc, FT-IR spectrum was taken on Perkin-Elmer Spectrum 100 and the scanning

electron microscopy (SEM) of samples were carried out on a TESCAN-VEG II electron microscope with an accelerating voltage of 15 KV.

### 3. RESULTS AND DISCUSSION

#### 3.1. IR

IR spectra of cobalt (III) hydroxide obtained from method I showed in figure 1. There are three strong bands due to the  $\nu(\text{-OH})$  modes, at  $3000\text{-}3500\text{ cm}^{-1}$  and  $1600\text{ cm}^{-1}$  due to  $\text{Co-ONO}$  or  $\text{H}_2\text{O}$ ,  $1400\text{ cm}^{-1}$  due to the stretching modes of  $\text{Co-ONO}$ ,  $600\text{ cm}^{-1}$  due to the bending modes of  $\text{Co-NO}$  and  $512\text{ cm}^{-1}$  due to the  $\text{M-O}$ .

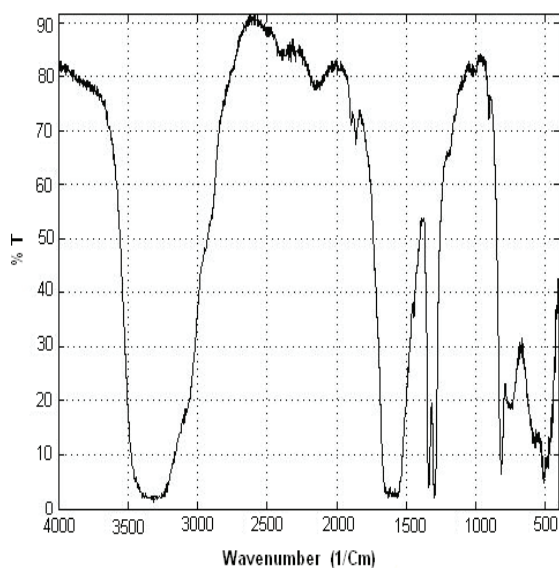


**Figure 1:** IR spectra of cobalt hydroxide.

In figure 2 showed IR spectra of tri cobalt tetra oxide ( $\text{Co}_3\text{O}_4$ ) which obtained from calcinations of cobalt hydroxide (a, b) and cobalt nitrate (c). There are two strong bands due to  $\nu(\text{Co-O})$  modes at  $\sim 662\text{ cm}^{-1}$  and  $\sim 576\text{ cm}^{-1}$  in figure 2, which is clear evidence for presence of crystalline  $\text{Co}_3\text{O}_4$  [5, 27, 29]. The IR spectrum of sample (b) displaying two distinct bands that originate from the stretching vibrations of the metal-oxygen bonds [30]. The first band at  $\sim 570\text{ cm}^{-1}$  is associated with the  $\text{OB}_3$  vibration in the spinel lattice where B denotes  $\text{Co}^{3+}$  in an octahedral hole. The second band at  $\sim 662\text{ cm}^{-1}$  is attributed to

the  $\text{ABO}_3$  vibration, where A denotes the  $\text{Co}^{2+}$  in a tetrahedral hole.

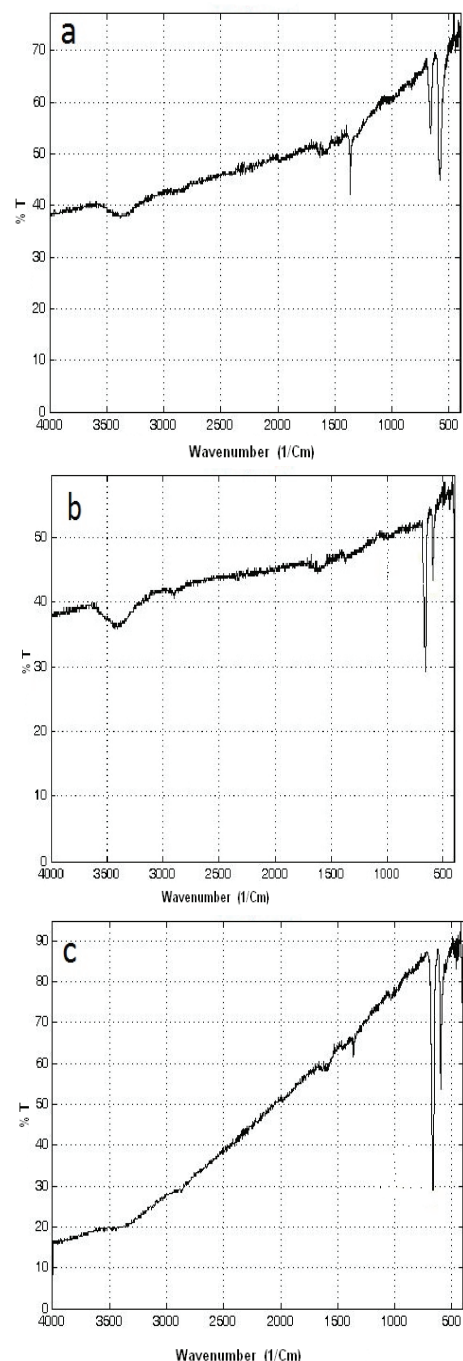


**Figure 2 (a, b, c):** IR spectra of tri cobalt tetra oxide ( $\text{Co}_3\text{O}_4$ ) obtained from cobalt hydroxide by calcinations (a) at  $300^\circ\text{C}$  for 1 hour, (b) at  $700^\circ\text{C}$  for 3 hours and (c) cobalt nitrate exposed to microwave energy.

The peaks at  $\sim 1600\text{ cm}^{-1}$  and  $\sim 3600\text{ cm}^{-1}$  should be assigned to  $-\text{OH}$  stretching and bending modes of water respectively which absorbed by the sample or KBr [31-33].

In figure 3 showed FT-IR spectra of cobalt oxide obtained from method III. There are two strong bands at  $\sim 564\text{ cm}^{-1}$  and  $\sim 661\text{ cm}^{-1}$  due to  $\nu(\text{Co-O})$  modes which indicates the presence of crystalline  $\text{Co}_3\text{O}_4$  and peaks at  $1100\text{ cm}^{-1}$  and  $3600\text{ cm}^{-1}$  should be assigned to  $\text{H}_2\text{O}$  absorbed by the sample or KBr [27].

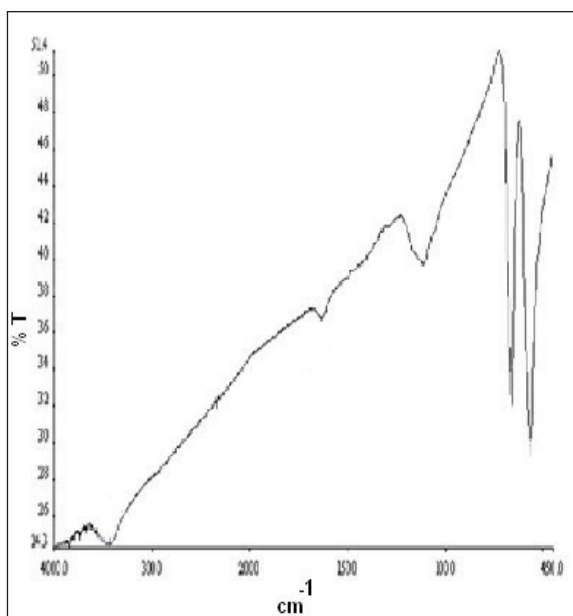


**Figure 3:** FT-IR spectra of  $\text{Co}_3\text{O}_4$  obtained from method III.

The IR spectra of three samples produced by method I are almost the same, hence two IR spectra illustrated in figure 2 indicated the formation of  $\text{Co}_3\text{O}_4$  at  $300^\circ\text{C}$  and  $700^\circ\text{C}$ . The IR spectrum of

sample 4 (Figure 2C) also conforms the formation of  $\text{Co}_3\text{O}_4$  by method II. The FT-IR spectra of the samples produced by method III also confirms the formation of  $\text{Co}_3\text{O}_4$ . Since the spectra of the two samples produced by method III are the same, then figure 3 demonstrated one spectra for both samples.

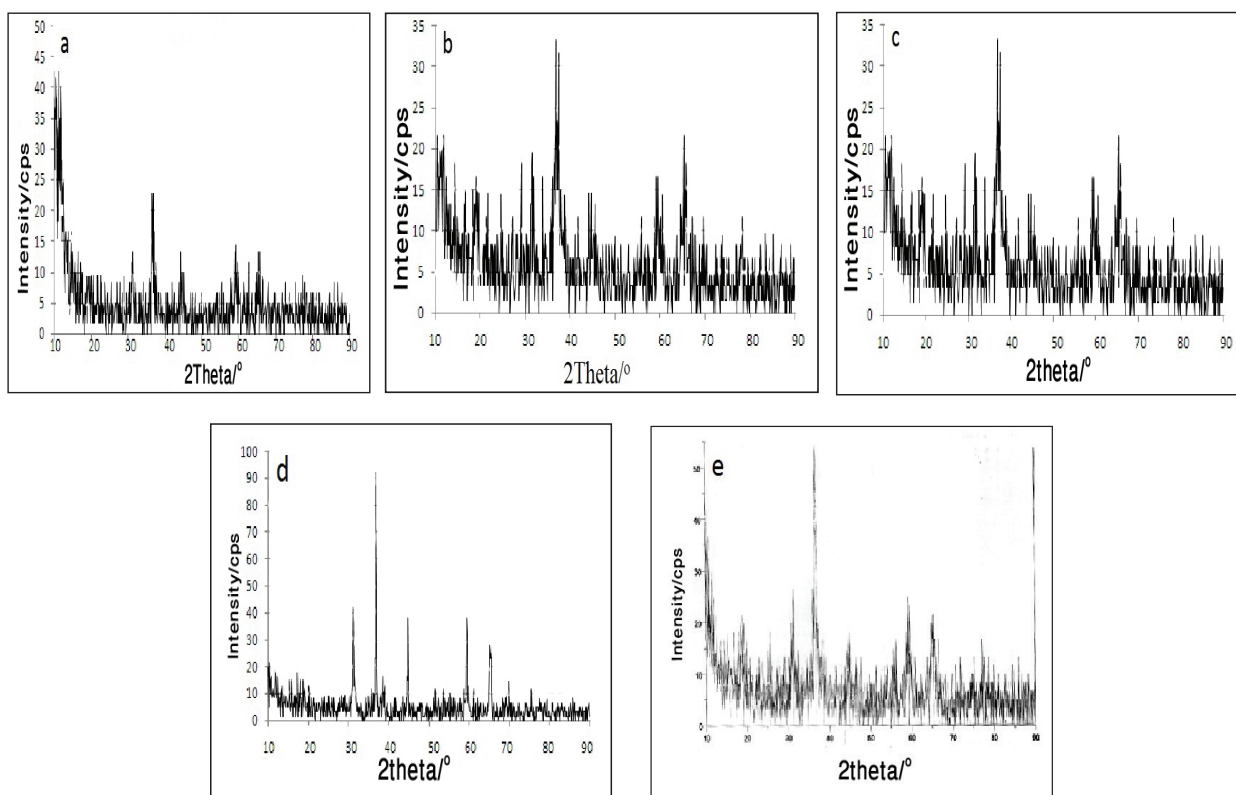
### 3.2. XRD

Figure 4 showed the XRD pattern of the final products obtained from methods I (b, c, d, e) and III (a). The XRD patterns indicate the monophasic fcc  $\text{Co}_3\text{O}_4$  phase is obtained by methods I and III. We can see that all samples obtained from different methods are  $\text{Co}_3\text{O}_4$ . As shown in figure 4 almost all of peaks intensities of (111), (220), (311), (222), (400), (422), (511), (440), can be perfectly indexed to a pure cubic phase (space group:  $\text{Fd}\bar{3}\text{m}$ ) of  $\text{Co}_3\text{O}_4$  ( $a=8.0840\text{\AA}$ ) reported in the literature (JCPDS 74-2120) [27]. The particle size of the investigated  $\text{Co}_3\text{O}_4$  solids was calculated from the line broadening analysis of some diffraction line of metal oxide phases using Scherrer equation [12]:  $D = k \cdot \lambda / \beta_{1/2} \cdot \cos(\theta)$  where  $k$  is the Scherrer's constant (0.89),  $D$  the mean crystalline diameter (nm),  $\lambda$  the X-Ray wavelength,  $\beta_{1/2}$  is the full width half maximum (FWHM) of the metal oxide diffraction peaks and  $\theta$  is the diffraction angle.

Inspection of these figures (Figure 4) revealed that the  $\text{Co}_3\text{O}_4$  solids prepared by different methods and calcined at  $300^\circ\text{C}$ ,  $500^\circ\text{C}$  and  $700^\circ\text{C}$  consisted of crystalline  $\text{Co}_3\text{O}_4$  phase which the quality of crystallinity increases by increase of calcinations temperature. The  $\text{Co}_3\text{O}_4$  nanoparticles prepared from method I and calcined at  $300^\circ\text{C}$ ,  $500^\circ\text{C}$  and  $700^\circ\text{C}$  have crystallite average size of 2 nm, 19 nm and 80 nm respectively which calculated from XRD pattern and Scherrer equation (Table 1).

**Table 1:** Variation of  $\text{Co}_3\text{O}_4$  nanoparticles size by increasing of the calcination temperatures

Sample	Temperature ( $^\circ\text{C}$ )	Size (nm)	
		XRD	SEM
Method I	300	2	25
	500	19	76
	700	80	93
Method III	400	18	70



**Figure 4 (a, b, c, d, e):** XRD patterns of  $\text{Co}_3\text{O}_4$  nanoparticles prepared by methods III (a) and I (b, c, d, e).

The XRD of three samples produced by method I and two samples by method III are illustrated by figure 4. The XRD of samples produced by method II were not taken because their size were above 100 nm that were not considered as good experimental results. The size of samples produced by method I and III were calculated by XRD patterns and scherrer equation are presented in table 1 which implies that the  $\text{Co}_3\text{O}_4$  nanoparticles produced by method I at 300°C is the best result obtained by this work.

### 3.3. SEM

The morphology and structure of the product were characterized by scanning electron microscopy (SEM). Figure 5 shows a typical SEM image of  $\text{Co}_3\text{O}_4$  nanoparticles with various size of 25 nm, 76 nm and 93 nm as increasing with different calcination temperatures of 300°C, 500°C, and 700°C respectively which clearly confirmed by

XRD results. Figure 5 (e, f, g) shows SEM images of micro-spheres obtained from the method II. The structure of the micro-spheres is shown obviously in Figure 5(f) which its diameter suggests to be about 1-1.5  $\mu\text{m}$ .

The morphology and structure of the samples produced by method I-III indicate that the smallest nanoparticle size is related to the sample produced by method I which calcinated at 300°C (Figure 5a) and the largest size is due to samples produced by method II (microwave method).

### 3.4. Catalytic activity of $\text{Co}_3\text{O}_4$ calcined at different temperature

Table 2 shows evolved oxygen volume as a function of time and catalytic activity of  $\text{Co}_3\text{O}_4$ . The catalytic activity calculated from  $a=k/(t.m)$  equation where a is the activity, k is a constant (mass of 5% hydrogen peroxide for production 100 ml.  $\text{O}_2$ ), t is reaction

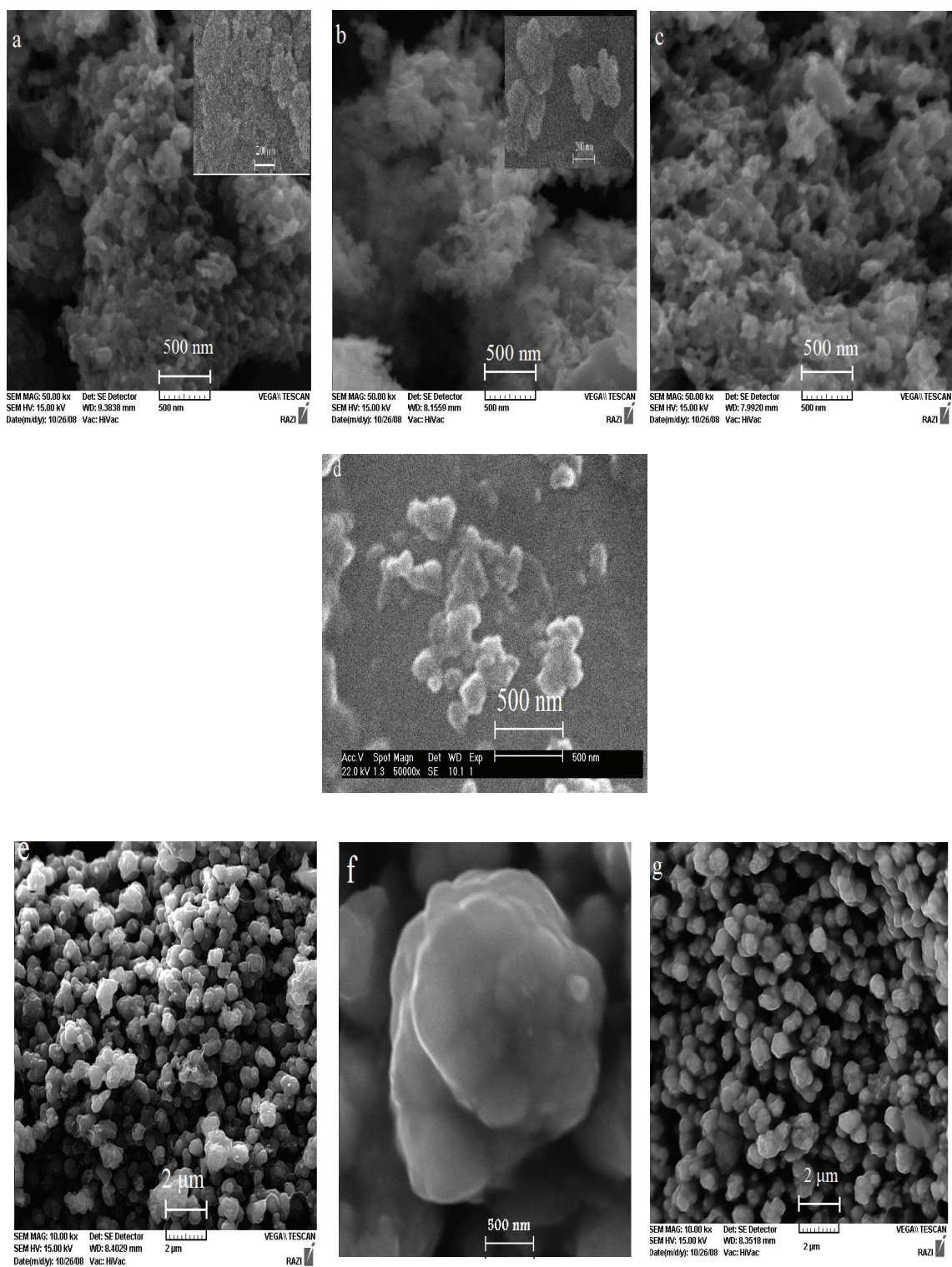


**Figure 5 (a, b, c, d, e, f, g):** SEM image of the  $\text{Co}_3\text{O}_4$  nanoparticles obtained from method I calcined at (a) 300°C, (b) 500°C and (c) 700°C, (d) method III calcined at 400°C for 24 hours and (e, f, g) micro-spheres powder obtained by method II.

**Table 2:** Variation of  $\text{Co}_3\text{O}_4$  nanoparticles catalytic activity by increasing of the calcination temperatures

Sample (Co-Precipitation method)	Temperature (°C)	Reaction time (s)	Catalytic activity ( $\times 100$ ) in $k=1$
$\text{Co}_3\text{O}_4$	300	25	40
$\text{Co}_3\text{O}_4$	500	65	15.4
$\text{Co}_3\text{O}_4$	700	140	7

time and  $m$  is mass of catalyst.

We saw that by increasing of calcinations temperature the catalytic activity of  $\text{Co}_3\text{O}_4$  nanoparticles was decreased.

#### 4. CONCLUSION

We have clearly demonstrated the importance of the method I for the preparation via precipitation method, and effect of calcination temperatures in morphologies of the  $\text{Co}_3\text{O}_4$  nanoparticles. It is concluded that the best method for preparation of  $\text{Co}_3\text{O}_4$  nanoparticles is the co-precipitation method and the best calcinations temperature is 300 °C. The microwave method is not a suitable method (method II) to prepare  $\text{Co}_3\text{O}_4$  nanoparticles. We found that at higher temperature, greater nanoparticles were produced which decreased the catalysts specific surface area and at the end decreased catalytic activity in decomposition of hydrogen peroxide.

#### 5. ACKNOWLEDGMENTS

This research effort is sponsored by I.H.U. and supported by a grant of department of chemistry and my colleagues for encouragement.

#### REFERENCES

1. J. Ahmed, T. Ahmed, K. V. Ramanujachary, S. E. Lofland, A. K. Ganguli, *Journal of Colloid and Interface Science*, Vol. 321, (2008), pp. 434-441.
2. H. Yang, Y. Hu, X. Zhang and G. Qui, "Materials Letters", Vol. 58, (2004), pp. 387-389.
3. Y. Chen, Y. Zhang and S. Fu, "Material Letters", Vol. 61, (2007), pp. 701-705.
4. V. R. Shinde, S. B. Mahadik, T. P. Gujar, C. D. Lokhande, *Applied Surface Science*, Vol. 252, (2006), pp. 7487-7492.
5. R. V. Narayan, V. Kanniah and A. Dhathathreyan, *J. Chem. Sci.*, Vol. 118, No. 2, (2006), pp. 179-184.
6. X. Liu, G. Qiu and X. Li, *Nanotechnology*, Vol. 16, (2005), pp. 3035-3040.
7. W. W. Wang, Y. J. Zhu, *Material Research Bulletin*, Vol. 40, (2005), pp. 1929-1935.
8. T. Li, S. Yang, L. Huang, B. Gu, Y. Du, *Chinese Phys. Lett.*, Vol. 21, (2004), pp. 966-969.
9. T. Li, S. Yang, L. Huang, B. Gu, Y. Du, *Nanotechnology*, Vol. 15, (2004), pp. 1479-1482.
10. C. Wang, H. Lin and C. Tang, *Catalysis Letters*, Vol. 94, (2004), pp. 69-74.
11. Y. Jiang, Y. Wu, B. Xie, Y. Xie, Y. Qian, "Materials Chemistry and Physics", Vol. 74, (2002), pp. 234-237.
12. N. R. E. Radwan, M. S. El-Shall, H. M. A. Hassan, *Applied Catalysis A: General* Vol. 331, (2007), pp. 8-18.
13. N. N. Greenwood, A. Earnshaw, (1984). "Chemistry of the elements." 4<sup>th</sup> ed., Pergamon Press, Oxford, pp. 1297.
14. A. Ruplecker, F. Kleitz, E. L. Salabas, F. Schuth, *Chem. Mater.*, Vol. 19, (2007), pp. 485-496.
15. L. X. Yang, Y. J. Zhu, L. Li, L. Zhang, H. Tong, W. Wang, et al., *Eur. J. Inorg. Chem.*, (2006), pp. 4787-4792.
16. Y. K. Liu, G. H. Wang, C. K. Xu, W. Z. Wang, *Chem. Commun.*, (2002), pp. 1486-1487.
17. T. He, D. R. Chen and X. L. Jiao, *Chem. Mater*, Vol.

- 16, (2004), pp. 737.
18. T. He, D. R. Chen and X. L. Jiao, *Chem. Mater*, Vol. 17, (2005), pp. 4023.
  19. H. Shao, Y. Huang, H. ee, Y. J. Suh and C. O. Kim, *J. Magn. Mater*, Vol. 304, (2006), pp. 28.
  20. L. D. Kadam, P. S. Patil, *Mater, Chem. Phys.* Vol. 68, (2001), pp. 225-232.
  21. R. N. Singh, J. F. Koenig, P. Chartier, *J. Appl. Electrochem.*, Vol. 137, (1990), pp. 1408-1413.
  22. M. Hamdani, J. F. Koenig, P. Chartier, *J. Appl. Electrochem.*, Vol. 18, (1988), pp. 568-576.
  23. P. N. Keng, J. F. Koenig, J. L. Gautier, P. Chartier and G. Poillerat, *J. Electroanalytical Chemistry*, Vol. 402, (1996), pp. 81-89.
  24. Y. Xuan, R. Liu, Y. Q. Jia, *Mater. Chem. Phys.* Vol. 53, (1998), pp. 256-261.
  25. B. B. Lakshmi, C. J. Patrissi C. R. Martin, *Chem. Mater*, Vol. 9, (1997), pp. 2544-2550.
  26. M. E. Baydi, G. Poillerat, J. L. Rehspringer, J. L. Gautier, J. F. Koenig and P. Chartier *J. Solid State Chem.*, Vol. 109, (1994), pp. 281-288
  27. L. Sun, H. Li, L. Ren and C. Hu, *Solid state Science*, Vol. 11, (2009), pp. 108-112.
  28. K. Venkateswara R.ao, C. S. Sunandana, *Solid State Communications*, Vol. 148, (2008), pp. 32-37.
  29. B. Pejova, A. Isahi, M. Najdoski, I. Grozdanov, *Materials Research Bulletin*, Vol. 36, (2001), pp. 161-170.
  30. C. W. Tang, C. B. Vang, S. H. Chien, *Thermochimica Acta*, Vol. 473, (2008), pp. 68-73.
  31. D. Zou, C. Xu, H. Luo, L. Wang, T. Ying, *Materials letters*, Vol. 62, (2008), pp. 1976-1978.
  32. J. A. Gaddsdén, (1975). "Infrared Spectra of Minerals and related Inorganic Compounds", 1<sup>st</sup> Ed., Butherworth, London.
  33. S. R. Ahmed, P. Kofinas, *J. Magn. and Magn. Mater*, Vol. 288, (2005).